

Exploring Semi-Supervised Learning for Online Mapping

Adam Lilja^{1,2} Erik Wallin^{1,3} Junsheng Fu² Lars Hammarstrand¹
¹Chalmers University of Technology ²Zenseact ³Saab AB
 {firstname.lastname}@{zenseact.com, chalmers.se, saabgroup.com}

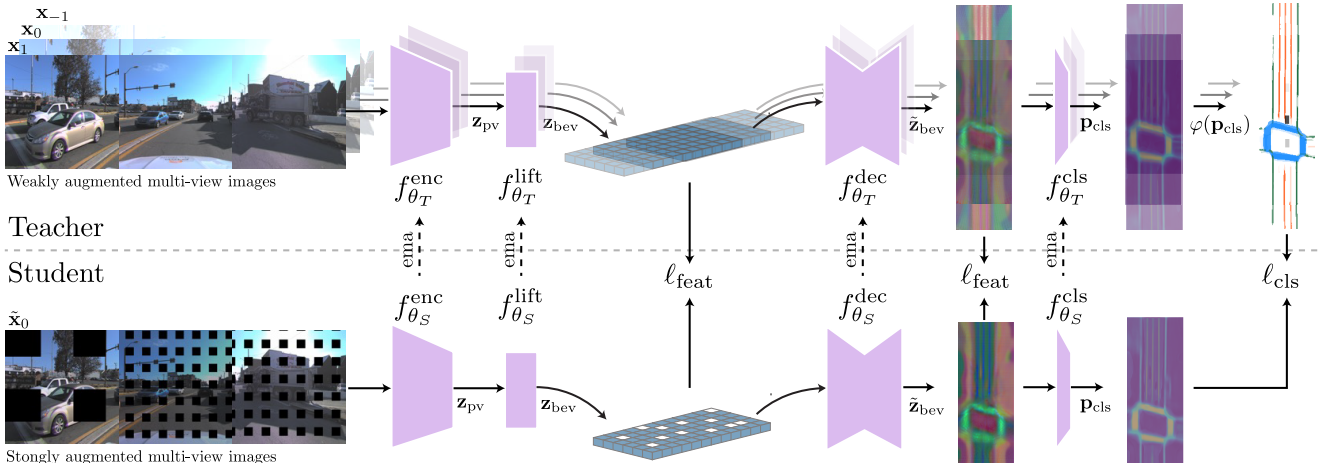


Figure 1. Semi-supervised learning framework for online mapping with temporal pseudo-label fusion. Our approach adapts the Teacher-Student paradigm to the online mapping domain while introducing a novel temporal fusion mechanism that aggregates pseudo-labels across multiple frames. We enable label-efficient learning from largely unlabelled datasets and strong generalization to unseen cities.

Abstract

The ability to generate online maps using only onboard sensory information is crucial for enabling autonomous driving beyond well-mapped areas. Training models for this task – predicting lane markers, road edges, and pedestrian crossings – traditionally require extensive labelled data, which is expensive and labour-intensive to obtain. While semi-supervised learning (SSL) has shown promise in other domains, its potential for online mapping remains largely underexplored. In this work, we bridge this gap by demonstrating the effectiveness of SSL methods for online mapping. Furthermore, we introduce a simple yet effective method leveraging the inherent properties of online mapping by fusing the teacher’s pseudo-labels from multiple samples, enhancing the reliability of self-supervised training. If 10% of the data has labels, our method to leverage unlabelled data achieves a 3.5x performance boost compared to only using the labelled data. This narrows the gap to a fully supervised model, using all labels, to just 3.5 mIoU. We also show strong generalization to unseen cities. Specifically, in Argoverse 2, when adapting to Pittsburgh, incorporating purely unlabelled target-domain data

reduces the performance gap from 5 to 0.5 mIoU. These results highlight the potential of SSL as a powerful tool for solving the online mapping problem, significantly reducing reliance on labelled data.

1. Introduction

Safe autonomous navigation requires accurately perceiving both dynamic traffic participants and static road infrastructure. Relying solely on pre-made offline High-Definition (HD) maps for the latter comes with difficulties, such as accurate localisation within the map, and the costs associated with building and keeping the maps up to date. The latter is significant for scaling Autonomous Driving (AD) beyond limited, well-mapped areas. Online mapping is an alternative and complementary approach, where onboard sensory data is used to produce a local up-to-date map of surrounding lane markers, road edges, and pedestrian crossings in real-time [25, 26].

Recent studies have shown that learning-based online mapping algorithms struggle to generalise to regions outside their training set, suggesting available data is insufficient for learning this complex task [28, 30, 40]. While collecting large amounts of AD data is relatively straightfor-

ward, the bottleneck lies in the effort labelling the data. Creating the necessary labels, *e.g.* 3D polylines for each lane divider, is generally time-consuming and costly. Therefore, we are interested in approaches utilizing a small amount of labelled data and a vast amount of unlabelled data to increase the generalisability in the online mapping task.

Other domains, such as image classification [43] and semantic segmentation [14], have addressed this problem setting through Semi-Supervised Learning (SSL) and shown strong capabilities. Recently, the interest in SSL for object detection has also gained traction and shown promising results [33, 51]. Some SSL techniques have been successfully adapted to the closely related domain of Bird’s Eye View (BEV) semantic segmentation of the combination of dynamic classes such as vehicles and pedestrians, and static classes including vegetation and drivable areas. However, the focus has been on *monocular* BEV segmentation where the teacher-student setup [43] has shown effectiveness [15, 60]. New challenges arise when multiple cameras are used as input, as creating 3D-consistent augmentations in this context proves difficult. For instance, the conjoint-rotation technique [60] is incompatible with our problem setup. Concurrent work [22] shows that randomly disabling camera feeds and applying BEV feature dropout as student augmentation techniques effectively enhance performance in a multi-camera setup. Despite these advances, there remains a gap in understanding how SSL components specifically interact in the context of online mapping, where the focus is exclusively on static classes rather than the mixed dynamic-static scenario addressed in prior work.

In this work, we identify key SSL approaches that excel in online mapping, both for learning with limited labels and for adapting models to new cities. As online mapping focuses solely on static classes, it allows us to exploit temporal consistency across frames. Building on this insight, we propose a label-efficient SSL method, illustrated in Fig. 1, that adapts the Teacher-Student paradigm to online mapping while introducing a novel temporal fusion mechanism. This mechanism aggregates pseudo-labels across multiple frames, improving their reliability and reducing noise. By leveraging large-scale unlabelled datasets, our approach significantly reduces dependence on labelled data while enabling strong generalization to unseen cities.

To summarize, we make four key contributions: 1) a comprehensive analysis of prevalent SSL techniques for online mapping, demonstrating which existing methods can significantly enhance performance. 2) combine SSL components into a robust method that maintains high performance levels across varying volumes of labelled data. 3) propose that the teacher model integrates information across multiple samples to improve pseudo-label accuracy. 4) demonstrate strong performance in domain adaptation when trained in one group of cities and evaluated in another.

2. Related Work

We explore semi-supervised learning and domain adaptation techniques specifically applied to online mapping. This section examines relevant prior work in these fields.

2.1. Semi-Supervised Learning

In SSL, costly labelled data is combined with inexpensive unlabelled data to train a model. There are two main approaches to this problem: single-stage training, where automatic ground truth labels are generated during training, *i.e.* using predictions from a single model or an ensemble of models as pseudo-labels [24, 41, 55], or a two-stage process starting with self-supervised pre-training followed by finetuning on the labelled data [5, 9, 21, 34]. This paper concentrates on the single-stage joint training approach, exploring critical design decisions and their impact on the performance of semi-supervised online mapping.

SSL has a rich history in image classification, with the teacher-student framework [43] being particularly influential. This framework involves a student network supervised by predictions from a teacher network. The teacher network shares the same architecture as the student but updates its weights as an exponential moving average (EMA) of the student’s weights. ReMixMatch [1] further feeds the teacher weakly augmented inputs, while the student receives strongly augmented inputs. Data augmentation is crucial in SSL [14, 45, 58] and these may differ from those suitable for fully supervised settings [58]. Commonly used augmentation strategies include RandAugment [11], CutOut [12], CutMix [53], and feature dropout [52].

FixMatch [41] further popularized *thresholding*, a technique where the student is supervised only with high-confidence pseudo-labels generated by the teacher. Numerous follow-up studies continue to demonstrate the strengths of this method [48, 52]. Another line of work in SSL involves adding self-supervised auxiliary tasks to improve performance, such as predicting the parameters of stochastic image transformations applied to unlabelled images [47, 54] or adding similarity loss of the features between the teacher and student models [10, 46].

Research in SSL has also been extended to BEV segmentation, considering a variety of classes such as car, truck, road, walkway, and vegetation [15–17, 60]. The teacher-student approach has, for instance, been adapted to monocular BEV segmentation, utilizing MSE losses for probability and feature similarity [15, 60]. Unlike in Perspective View (PV) semantic segmentation, where a variety of augmentations are permissible, the augmentations applied in BEV segmentation must maintain 3D consistency. *E.g.*, methods such as randomly cropping and resizing the PV input image for BEV segmentation can break geometric consistency in the BEV plane. One augmentation with geometric consistency is the conjoint rotation introduced in [60] where both

images and BEV pseudo-labels are rotated around the upward axis. However, this technique is limited to monocular camera setups, as any augmentation affecting the 3D geometry must maintain 3D consistency across all cameras.

Our setup closely resembles the concurrent work of PCT [22], which proposes SSL on multi-view images using a teacher-student framework inspired by [52]. They introduce camera dropout augmentation, where one or more camera images are omitted for the student model, and leverage BEV feature dropout. Additionally, they use pre-trained models to generate PV semantic segmentation and depth pseudo-labels. In contrast, our work focuses on SSL methods that do not rely on additional pre-trained networks for pseudo-labeling. Another key distinction is that, unlike BEV segmentation, which includes dynamic object classes, online mapping is concerned solely with stationary elements.

2.2. Domain Adaptation

Unsupervised domain adaptation (UDA) is closely related to SSL, and throughout this paper, we will use the terms interchangeably. In UDA, the unlabelled data comes from a target domain that differs from the labelled source domain. The goal of UDA is to achieve strong performance in unseen environments, which is particularly critical for online mapping, where models must perform well in cities they have never been trained on – a problem often overlooked in prior work [28]. Similar to SSL, many UDA techniques rely on self-training with a teacher-student setup and have also demonstrated strong results across various UDA settings [61]. A dominant approach for perspective view semantic segmentation in the image plane for AD involves augmenting data by mixing crops of labelled and unlabelled samples [7, 44]. However, such augmentations are poorly suited for online mapping, as they fail to maintain consistency across multiple camera views, a key requirement in our setting. In this work, we focus on self-training for UDA in online mapping, emphasizing its importance in adapting to unseen cities – a fundamental challenge for real-world deployment.

2.3. Online Mapping

Recently, significant progress has been made in the field of online mapping, leading to the development of two primary approaches: segmentation-based methods [13, 25, 37, 50] and vector-based methods [6, 26, 27, 32] where the key difference lies in the output representation. Segmentation-based methods rasterize a region from a Bird’s Eye View and classify each cell, typically using a CNN [13, 25, 38]. The vector-based methods predict vectors with connected points, representing a polyline for each object, typically using a DETR-like [4] transformer decoder [26, 27, 57].

Both approaches encode input images using a neural network and transform the features into BEV using a core tech-

nique known as *lifting*. For instance, LSS [39] learns a categorical depth distribution for each pixel and use it to weigh how much the corresponding PV feature should influence the corresponding BEV-cell.

Previous works have highlighted a performance drop as the domain gap between training and evaluation data increases. Particularly in the context of geographical distribution shifts [28, 40], and driving scenario shifts [30]. Our focus is on the effects of SSL approaches, and for this work, we choose a segmentation-based method, as its formulation aligns more naturally with existing SSL and UDA techniques.

3. SSL for Online Mapping

Our work focuses on leveraging SSL to maximize the effectiveness of unlabelled data in online mapping. In this context, we assume that we have a small set of labelled data $\mathbf{X}_L = \{\mathbf{x}_i, \mathbf{y}_i\}_{i=1}^{n_l}$, for which ground truth map \mathbf{y}_i is available, and a large set of unlabelled images $\mathbf{X}_U = \{\mathbf{x}_i\}_{i=1}^{n_u}$ without ground truth annotations. The latter is assumed to be collected in areas separate from the labelled set, but using the same camera setup. Further, the relative pose of the vehicle in the sequences is assumed to be known.

Using the labelled data, the student is trained in an ordinary supervised manner by minimizing a supervised loss $\ell_{\text{sup}}(\mathbf{x}_i, \mathbf{y}_i)$, e.g., cross-entropy, DICE [42], or Focal Loss [29]. Effectively using the unlabelled data is more challenging as we do not have access to a ground truth map for this area, and several design choices must be made. To understand how to apply SSL methods in the context of online mapping, we explore the impact of these choices using a well-established segmentation-based online mapping architecture. Figure 1 shows an overview of the SSL training scheme, and in this section, we provide the details of the online mapping architecture, the prevalent SSL techniques we employed, and our proposed multi-step teacher fusion approaches.

3.1. Online mapping architecture

As we are mainly interested in the effects of SSL approaches, we choose to use a typical map segmentation architecture [25, 37, 56] such as Fig. 1 illustrates. The multi-view images, \mathbf{x} , are encoded by a neural network $\mathbf{z}_{\text{pv}} = f_{\theta}^{\text{enc}}(\mathbf{x})$ and lifted to BEV features as $\mathbf{z}_{\text{bev}} = f_{\theta}^{\text{lift}}(\mathbf{z}_{\text{pv}})$. Then, another neural network decodes the BEV features $\tilde{\mathbf{z}}_{\text{bev}} = f_{\theta}^{\text{dec}}(\mathbf{z}_{\text{bev}})$. Final class probabilities are predicted through a classification head $\mathbf{p}_{\text{cls}} = f_{\theta}^{\text{cls}}(\tilde{\mathbf{z}}_{\text{bev}})$, where \mathbf{p}_{cls} comprise the independent probability of each map grid cell containing a lane delimiter, road edge, or pedestrian crossing. As such, the online map is treated as a multi-label semantic segmentation problem. The complete architecture can be described as $\mathbf{p}_{\text{cls}} = F_{\theta}(\mathbf{x})$.

3.2. Semi-supervised training scheme

The primary training methodology adopted in this work is based on the Mean Teacher framework [43]. As illustrated in Fig. 1, we use two identical network architectures: a teacher-version, parameterized by θ_T , and a student-version, described by θ_S . In this setup, only the student is trained directly from data, \mathbf{X}_L and \mathbf{X}_U . The teacher weights are updated after each training step using an exponentially moving average (EMA) of the student, $\theta_T \leftarrow \alpha\theta_T + (1 - \alpha)\theta_S$, where α is the keep rate.

We investigate two common forms of SSL schemes, pseudo-labelling and consistency regularization through feature similarity. The first follows the approach in [1, 41, 43, 61], where the student is trained using pseudo-labels (pseudo-maps for our setting) predicted by the teacher. The teacher network receives a weakly augmented version of the input images \mathbf{x} (and possibly a set of additional surrounding data samples, Sec. 3.6), for which it predicts a pseudo-map $\hat{\mathbf{y}} = \varphi(F_{\theta_T}(\mathbf{x}))$. Here, $\varphi(\cdot)$ is used to decide/design suitable pseudo-labels based on the predicted class probabilities, *e.g.*, thresholding and/or sharpening (see Sec. 3.4). The student receives a strongly augmented version of the same sample $\tilde{\mathbf{x}}$ (see Sec. 3.3) and is trained to make consistent class predictions with the teacher model through a pseudo-label loss $\ell_{\text{cls}}(F_{\theta_S}(\tilde{\mathbf{x}}), \varphi(F_{\theta_T}(\mathbf{x})))$ similar to ℓ_{sup} .

The feature similarity supervision, on the other hand, enforces consistency between intermediate features for the teacher and student models. More formally, we train the student network to minimize a feature similarity loss, using *e.g.* Mean Squared Error or Cosine Similarity, $\ell_{\text{feat}}(\mathbf{z}_{\theta_T}(\mathbf{x}), \mathbf{z}_{\theta_S}(\tilde{\mathbf{x}}))$. Here, \mathbf{z}_{θ_T} and \mathbf{z}_{θ_S} are intermediate features on the same level, *e.g.* \mathbf{z}_{bev} or $\tilde{\mathbf{z}}_{\text{bev}}$, using teacher and student models, respectively. In contrast to the pseudo-label training, feature similarity is insensitive to errors in teacher predictions as we avoid any label decisions. Instead, we enforce the representation of the same scene to be consistent in both models and is further discussed in Sec. 3.5.

In sum, the total training loss for the student is

$$\ell = \sum_{\mathbf{x}_i \in \mathbf{X}_L} \ell_{\text{sup}}(\mathbf{x}_i, \mathbf{y}_i) + \sum_{\mathbf{x}_i \in \mathbf{X}_U} \omega_{\text{cls}} \ell_{\text{cls}}(F_{\theta_S}(\tilde{\mathbf{x}}_i), \varphi(F_{\theta_T}(\mathbf{x}_i))) + \omega_{\text{feat}} \ell_{\text{feat}}(\mathbf{z}_{\theta_S}(\tilde{\mathbf{x}}_i), \mathbf{z}_{\theta_T}(\mathbf{x}_i)),$$

where ω_{cls} and ω_{feat} are hyperparameters controlling the relative importance of the respective loss.

3.3. Augmentations

Strong augmentation techniques applied to the student’s input are essential for effective learning [58]. Therefore, we explore various data augmentation strategies that preserve the scene’s geometry, as discussed in Sec. 2.1. Specifically, we employ photometric augmentations, CamDrop [22], CutOut [12], and BEVDrop [52]. *Photometric augmentations* introduce random variations in appearance by

adjusting brightness, contrast, saturation, hue, and color conversion, as well as performing random channel swaps. *CamDrop* augmentation simulates missing camera views by completely removing the input from one or more cameras. The dropped camera’s field of view is also masked from the loss. *CutOut* randomly masks out rectangular regions in the input images while *BEVDrop* operates on the BEV feature representation randomly setting certain grid cells to zero.

3.4. Sharpening and thresholding

Predictions from the teacher are often refined through thresholding and sharpening before being used as pseudo-labels for the student. Thresholding keeps only predictions above some confidence level, whereas sharpening scales the predicted distribution to alter the confidence of the pseudo-label. For thresholding, we adapt FixMatch [41], *i.e.*, only predictions exceeding a fixed confidence threshold contribute to the loss. For sharpening, we explore two techniques: (1) *hard* pseudo-labeling where teacher predictions are reduced to its argmax [23, 41], and (2) temperature sharpening, where the predicted logits are rescaled through division by a temperature parameter (denoted T in [2, 18]) before applying sigmoid to get a *soft* pseudo-label. More formally, splitting up the classification head, $\mathbf{p}_{\text{cls}} = f_{\theta}^{\text{cls}}(\tilde{\mathbf{z}}_{\text{bev}}) = \sigma(f_{\theta}^{\text{logits}}(\tilde{\mathbf{z}}_{\text{bev}}))$, we have the intermediate logits $\hat{\mathbf{z}}$. Sharpening using the hyperparameter T is then defined as $\hat{\mathbf{z}}_{\text{sharpen}} = \hat{\mathbf{z}}/T$. For $0 < T < 1$ the certainty is artificially increased, *i.e.* $\hat{\mathbf{z}}_{\text{sharpen}} > \hat{\mathbf{z}}$. Conversely, $T > 1$ decreases the pseudo-label certainty.

3.5. Feature Similarity

To further enhance consistency between the teacher and student networks, we impose feature similarity constraints at the BEV feature level. A key consideration in this approach is selecting both the loss function and the feature level at which to apply the constraint. We explore two candidate feature levels for enforcing similarity: *Early* BEV representation (\mathbf{z}_{bev}) – immediately after the lifting process, capturing the initial transformation of multi-view image features into the BEV space. *Late* BEV representation ($\tilde{\mathbf{z}}_{\text{bev}}$) – just before the final decoding step, where the network has refined its scene understanding. By constraining intermediate features to be consistent, we encourage the student model to align with the teacher’s representations without relying on explicit pseudo-labels. However, excessive weighting of the feature similarity loss may destabilize training, potentially leading to trivial solutions where the student merely replicates the teacher’s features instead of learning meaningful representations.

3.6. Teacher Fusion

Unlike BEV segmentation, which includes dynamic classes, all categories in online mapping are stationary. This key

Table 1. Performance (mIoU) of various augmentations. Using multiple augmentations yields strong results, significantly outperforming no augmentations. We also note that CutOut [12] works better than CamDrop [22] for online mapping.

Augmentation				Label utilisation	
Photom.	CamDrop	CutOut	BEVDrop	2.5%	10%
				12.1 \pm 0.6	21.3 \pm 0.2
✓				13.3 \pm 0.6	32.0 \pm 0.1
✓	✓			21.9 \pm 1.0	31.9 \pm 0.1
✓		✓		24.4 \pm 1.2	33.9 \pm 0.2
✓		✓	✓	25.5 \pm 0.7	34.3 \pm 0.1

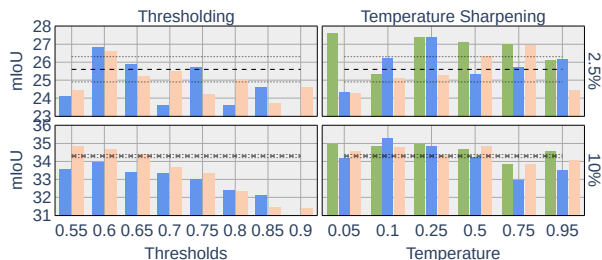


Figure 2. No thresholding, soft MixMatch [2], and hard FixMatch[41] thresholding utilising 2.5% and 10% of the labels. $\bar{Baseline}$, mean and std., use neither thresholding nor sharpening.

distinction, combined with the fact that sensor data is collected in sequential frames with known ego vehicle motion, enables novel strategies not commonly explored in other domains. We propose to leverage this by fusing pseudo-labels from the teacher across multiple nearby frames.

As illustrated in Fig. 1, predictions from both past and future frames can be transformed into the current coordinate frame using the known ego motion. By selecting only the most confident teacher predictions from any of these frames, we provide the student with a more complete and accurate map representation. This approach is particularly beneficial for improving predictions in regions far from the ego vehicle, where accuracy tends to degrade [13]. We also explore feature fusion by averaging overlapping BEV feature representations (\tilde{z}_{bev}) across multiple frames.

To ensure that additional frames contribute meaningful new information, we randomly sample them at varying distances relative to the current frame. This strategy mitigates issues with strictly time-based selection, such as: ego vehicle being stationary, which provides no new information, and the vehicle moving at high speeds, leading to minimal spatial overlap between frames.

4. Experiments

To explore the effectiveness of SSL for online mapping, we describe the experimental setup in Sec. 4.1 and conduct comprehensive ablation studies in Sec. 4.2 to evaluate the contribution of each component. Building on these results, we further evaluate the performance in Sec. 4.3.

Table 2. mIoU for sharpening methods using threshold 0.6. Neither soft MixMatch [2] nor hard thresholding FixMatch[41] show significantly impact over using no thresholding

Technique	Label utilisation			
	Thr.	Hard	2.5%	10%
			25.5 \pm 0.7	34.3 \pm 0.1
✓			25.1 \pm 1.3	33.9 \pm 0.1
✓	✓		25.4 \pm 0.8	34.6 \pm 0.1

4.1. Experimental Setup

We employ a ResNet50 [20] as image encoder f_{θ}^{enc} , LSS [39] for lifting features to BEV f_{θ}^{lift} , and a lightweight convolutional bottleneck decoder inspired by [19] as f_{θ}^{dec} . We perform multi-label prediction for pedestrian crossings, lane dividers, and road boundaries and use Focal Loss [29] as the supervised loss ℓ_{sup} on the labelled dataset and ℓ_{cls} for the unlabelled data. The region of interest follows [31] spanning $\pm 45m$ longitudinally and $\pm 15m$ laterally. Each cell has a side length of 0.3m. For brevity, we report the mean Intersection over Union (mIoU) across these three classes. To account for the stochasticity in the results from individual runs, we either report the mean and standard deviation of the mIoU for three runs with the same hyperparameters or multiple nearby values of the hyperparameter. We choose to follow [15] and use unlabelled weight $\omega_{cls} = 1$. We follow [22] and linearly ramp-up ω_{cls} , and when applicable ω_{feat} , over the first third of the training. Unless stated otherwise, no thresholding or sharpening is used in the experiments. For the CutOut augmentation, we remove 25% of the image, and for BEV feature dropout (BEVDrop) we follow [22, 52] and drop 50% of the features. The models, unless stated otherwise, are trained and evaluated using the Argoverse 2 (AV2) dataset [49] with the geographically disjoint splits proposed by [28] using surround-view camera images as input and use the provided HD maps as labels. We generally experiment using two utilisation rates of labelled data, namely 2.5% and 10%, corresponding to 18 and 70 labelled sequences respectively.

4.2. Exploration

We explore different SSL approaches outlined in Sec. 3 to show their effectiveness for segmentation-based online mapping.

Augmentations: We evaluate various strong augmentation strategies for the student model, as discussed in Sec. 3.3. The results in Tab. 1 demonstrate that increasing the difficulty of the task for the student model is crucial also for online mapping. With 10% label utilisation, Photometric augmentation alone is sufficient for significant model improvement. However, with 2.5% label utilisation, additional augmentations are required. For both label utilisation ratios, applying Photometric, CutOut, and BEVDrop yields

the best performance, and we adopt this configuration as the *Baseline* in further experiments. Specifically, we observe a significant performance improvement, with mIoU increasing from 12.1 to 25.5 for the 2.5% label utilisation and 21.3 to 34.3 for the 10% label utilisation. Furthermore, contrary to the findings in [22], we find that removing parts of the images, *i.e.* CutOut, yields better performance than dropping an entire camera and masking its field of view in the loss, as done with CamDrop.

Sharpening and Thresholding: The effects of sharpening and thresholding are illustrated in Fig. 2. As shown to the left, supervising with the most confident pseudo-labels does not yield significant performance improvements. However, using a low confidence threshold provides a slight boost in performance, and we set the threshold to 0.6 for subsequent experiments. The right plot shows the impact of sharpening. While sharpening can lead to minor improvements, the gains are marginal and introduce an additional hyperparameter, making it less appealing for our setting. Tab. 2 presents results across multiple runs, comparing hard and soft label supervision. Overall, these techniques have limited impact on online mapping, contrasting findings in other domains where sharpening has been highly effective—typically when used alongside high thresholds [41].

Feature Consistency: We compare the performance using Mean Squared Error (MSE) and Cosine Similarity (COS) losses with $\omega_{\text{cls}} = 1$ and varying feature loss weight ω_{feat} . In Fig. 3 the results are displayed using features from before or after the BEV decoder f_{θ}^{dec} as inputs to ℓ_{feat} . When utilizing 2.5% of the labels the results are noisy, and no clear benefit from the additional supervision is observed across the setups. However, for the 10% label utilisation, *late* COS consistency provides a slight performance gain and demonstrates greater stability than the MSE loss. While prior BEV segmentation works opted to use MSE [15, 60], we believe COS to be the better choice for our setting.

Teacher Fusion: To enhance pseudo-labels, we propose to fuse teacher predictions from multiple samples. We use two additional samples, as we empirically found, see Sup. mat. Sec. 6, that adding more samples does not provide further benefits but makes training slower due to the additional inference costs. Therefore, we focus on examining the influence of the maximum distance to these additional samples. The results in Fig. 4 show that even our simple fusion of predicted probabilities generally improves performance, both with and without thresholding. The fusion of BEV features, on the other hand, shows no significant benefit. For 2.5% label utilisation we observe that increasing the range to above 20m is required to improve performance, whereas for 10% the maximum range is not as important. In further experiments, we will use 30m as it works well for both utilisation ratios. While the simple probability fusion strategy yields strong results, exploring more advanced fusion

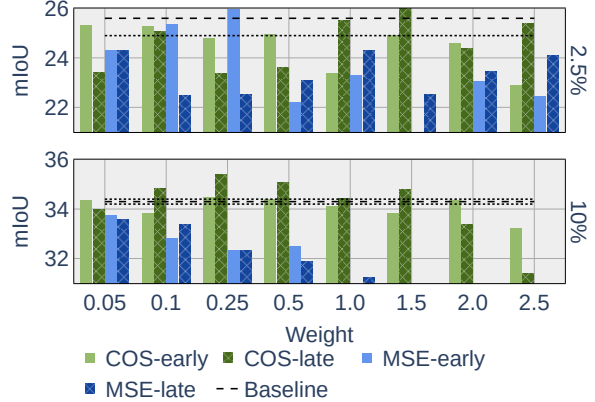


Figure 3. Feature Similarity using Mean Square Error following [60] and Cosine Similarity following [46] varying ω_{feat} . *Baseline* refers to no feature similarity while *early* and *late* refers to using BEV features before or after BEV processing f_{θ}^{dec} in Fig. 1.

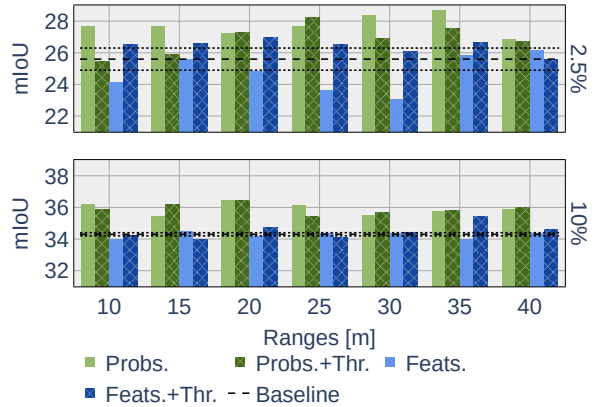


Figure 4. Teacher Fusion across varying maximum ranges from the current sample. Fusing the probabilities yields consistent improvements over the *Baseline*, without any fusion.

techniques is a promising avenue for future research.

Combining Components: Building on the above results, we further explore how these components interact in SSL for online mapping. Starting with the teacher-student setup as a *Core* we incrementally add components and evaluate their impact on performance. Here, we add strong augmentations to the student, *+Augs*, with Photometric, CutOut, and BEVDrop. Teacher fusion, *+Fusion*, is used with a maximum range of 30m. The Cosine feature similarity loss is incorporated under *+Featsim* with a weight of $w_{\text{feat}} = 0.25$. Additionally, a threshold of 0.6 is used without any temperature sharpening in *+Thr*, and hard pseudo-labeling is further added and denoted with *+Hard*.

The results in Tab. 3 demonstrate that combining components leads to further increased performance. Adding strong augmentations to the student yields a significant performance boost, as does further incorporating teacher fusion. Together these contribute to mIoU gains of 16.1 and 15.1 for 2.5% and 10% respectively. When combined with Fusion, feature similarity slightly improves performance for

Table 3. mIoU when incrementally adding SSL components.

Lbl. Util.	Core	+Augs	+Fusion	+Featsim	+Thr.	+Hard
2.5%	12.1 \pm 0.6	25.5 \pm 0.7	28.2 \pm 0.7	29.0 \pm 0.6	29.4 \pm 0.3	29.3 \pm 1.1
10%	21.3 \pm 0.2	34.3 \pm 0.1	36.4 \pm 0.2	36.4 \pm 0.5	36.8 \pm 0.2	36.7 \pm 0.3

Table 4. mIoU when using DINOv2 backbone adding SSL.

Backbone	SSL	Label utilisation	
		2.5%	10%
ResNet50		7.5 \pm 0.9	10.6 \pm 0.2
DINOv2		11.3 \pm 0.6	17.3 \pm 0.4
ResNet50	✓	29.4 \pm 0.3	36.8 \pm 0.2
DINOv2	✓	28.7 \pm 0.9	33.2 \pm 0.2

2.5% labelled data, but has no impact for 10%. Finally, applying thresholding yields a modest improvement for both ratios, while using the hard pseudo-labels does not contribute further. These results underscore the importance of conducting ablation studies across different labelled data ratios, as the impact of various modules can vary depending on the amount of labelled data.

4.3. Putting SSL to the Test

Building on the design choices made above, we aim to further verify the strengths of our proposed SSL scheme. Using the parameters from Sec. 4.2, our proposed method includes strong augmentations, teacher fusion, cosine feature similarity, and thresholding. As before, we report the mean and standard deviation; however, in this case, we select the best-performing model on the validation set and evaluate it on the test set. The performance is compared by utilizing both unlabelled and labelled data with the SSL-scheme versus using *only* the labelled data in a supervised setting. First, we compare our SSL scheme against swapping the backbone for a vision foundation model. Next, we evaluate the robustness of our method across different online mapping architectures. We then examine its scalability with varying amounts of labelled data and demonstrate the method’s effectiveness for domain adaptation.

Comparing with pre-training: We substitute the ImageNet pre-trained ResNet50 with DINOv2 [36] vision foundation model, which leverages pre-training on a substantially larger dataset. Although DINOv2’s size makes it impractical for vehicular deployment, it demonstrates performance improvements in Tab. 4. Nevertheless, a significant performance gap persists when comparing DINOv2 without SSL to our SSL approach. Notably, integrating our SSL scheme with the DINOv2 backbone eliminates this gap, underscoring the effectiveness of our approach.

Robustness to model architecture: We apply our proposed SSL setup to state-of-the-art online mapping models. As shown in Fig. 5, various architectures—including CVT [59], IPM [19], GKT [8], and LSS [39] – all benefit significantly from the SSL scheme. LSS achieves the highest overall performance, with a 3.9x and 3.5x boost when 2.5% and

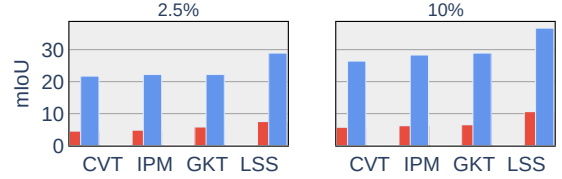
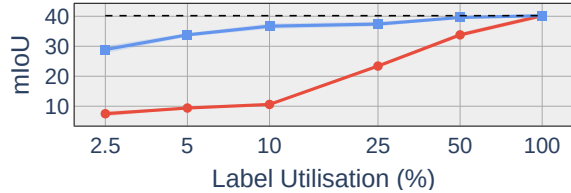
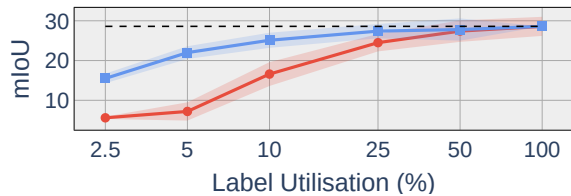


Figure 5. Multiple SOTA online mapping methods benefit from the SSL-scheme compared to the supervised training.



(a) Argoverse 2



(b) nuScenes

Figure 6. Test performance (mIoU) across utilising various amount of the labelled nuScenes data. All data is used as unlabelled for all runs. Training with unlabelled data using the SSL-scheme consistently improves performance compared to only using supervised training across all label utilizations.

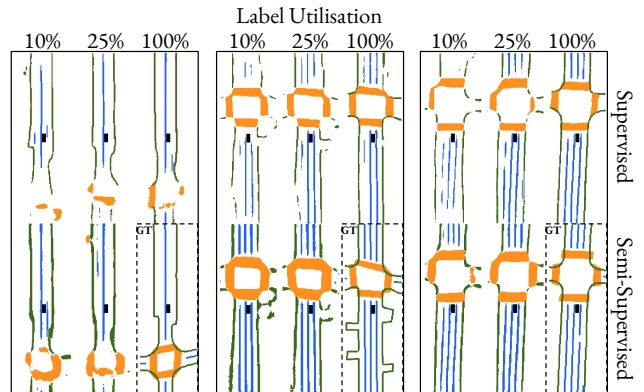


Figure 7. Qualitative results with varying amounts of labelled data. Predictions are shown for models trained with 10%, 25%, and 100% of the labelled data, using both standard supervised training and our proposed SSL approach.

10% of the data have labels, respectively. While *e.g.* CVT performs slightly worse overall, it sees even greater relative improvements, with performance increasing by 4.8x and 4.6x under the same label utilizations.

Scalability: We conduct experiments on AV2 [49] and nuScenes [3], with the same hyperparameters except for learning rate and weight decay. Our experiments range from using the labels from the full dataset, corresponding to 700 sequences, down to just 18 sequences at 2.5% utili-

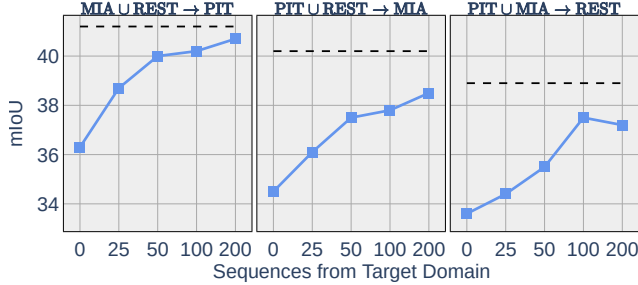


Figure 8. Adapting to new cities for AV2. Adding unlabelled sequences with the SSL-scheme from the target domain enhances performance in the target city. When adapting to Pittsburgh, the gap is almost completely closed to using all target labels.

sation. Figure 6 shows how our proposed SSL method and its supervised counterpart scale with varying amounts of labelled data. For the supervised models, performance decreases rapidly as the amount of (labelled) data is reduced. In the most label-scarce setting, having access to 2.5% of the labels, models trained solely on labelled sequences perform poorly, with mIoU dropping to 7.5 for AV2 and 5.6 for nuScenes. Incorporating unlabelled data with our proposed approach yields substantial performance boosts across all labelled data utilisation ratios. Leveraging unlabelled data with the SSL-scheme dramatically improves performance to 28.9 and 15.5 mIoU for the respective datasets.

If 10% of the data has labels, our method achieves a 3.5x performance boost compared to only using the labelled data. This narrows the gap to a fully supervised model that uses all labels, to just 3.5 mIoU on AV2. For nuScenes, the performance boost is 1.5x, and the remaining gap to when all labels have been used is reduced to 3.5 mIoU.

To provide visual context for these quantitative improvements, Fig. 7 shows predictions from models trained only on labelled data against those trained with both labelled and unlabelled data. The predictions are noticeably more stable and reliable when using our semi-supervised method, aligning with the quantitative improvements reported above.

City Adaptation: We assess our method’s ability to adapt to new cities using the AV2 Far Extrapolation splits from [28] and the Boston-to-Singapore split from [35] for nuScenes. Our approach utilises all labelled data from the source cities while gradually incorporating unlabelled data from the target cities, ensuring geographic separation from the test set. As shown in Fig. 8 and Fig. 9 for AV2 and nuScenes, respectively, we find that even without labelled data from the target city, performance improves significantly by utilizing its unlabelled data. The domain gap between Boston and Singapore in nuScenes is substantial, making adaptation more challenging than in AV2, where all data comes from US cities. Notably, performance improves as more unlabelled sequences from the target domain are added, suggesting that additional unlabelled data could further enhance results. For smaller domain gaps, such as

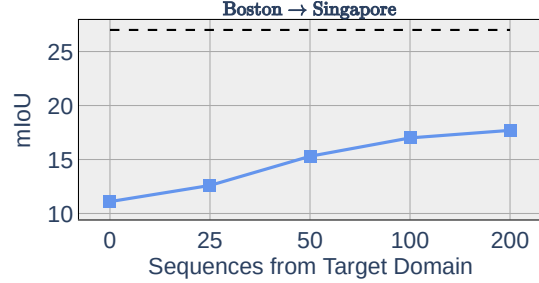


Figure 9. City adaptation from Boston to Singapore on nuScenes. While performance naturally is lower than using all Singapore labels, incorporating unlabelled sequences using the SSL-scheme helps improve the model’s performance when labelled data is only available from Boston.

adapting to Pittsburgh in AV2, our method nearly matches the performance of a fully supervised model, with only a 0.5 mIoU difference. For larger domain gaps, such as Boston to Singapore, our method boosts mIoU from 11.1 to 17.0 when using 100 unlabelled sequences from Singapore. However, a substantial gap remains in cases of large domain shifts, posing a key challenge for future research.

5. Conclusion

This paper draws inspiration from SSL techniques in other domains, demonstrating their effectiveness for segmentation-based online mapping. We show that applying photometric, CutOut, and BEVDrop augmentations in a teacher-student setup already performs well. When combined with our proposed multi-step fusion, and feature similarity constraints we show an additional performance boost.

Using the proposed SSL-scheme, we show that incorporating unlabelled data substantially improves performance on both AV2 and nuScenes compared to relying solely on labelled data. For example, if 10% of the data has labels, the SSL-approach to leverage unlabelled data achieves a 3.5x performance boost compared to only using the labelled data, narrowing the gap to a fully supervised model that uses all labels to just 3.5 mIoU. We also show strong generalization to unseen cities and believe that additional unlabelled data could further enhance the domain adaptation results. Still, when adapting to Pittsburgh (AV2), incorporating purely unlabelled target-domain data reduces the performance gap from 5 to just 0.5 mIoU.

In summary, efficiently leveraging both labelled and unlabelled data is crucial for advancing online mapping. While this work does not explore all existing SSL methods, it provides a foundation for understanding key SSL methods in this context and highlights their potential. We hope this study inspires further research in teacher fusion strategies, self-supervised pre-text tasks, and broader semi-supervised learning approaches to enhance online mapping performance further.

Acknowledgements

We want to express our sincere gratitude to Adam Tonder-ski, Georg Hess, William Ljungbergh, Carl Lindström, Ji Lan, and Erik Stenborg for their continuous support and invaluable discussions. This work was partially supported by the Wallenberg AI, Autonomous Systems and Software Program (WASP) funded by the Knut and Alice Wallenberg Foundation. Computational resources were provided by the National Academic Infrastructure for Supercomputing in Sweden (NAISS) at [NSC Berzelius](#) and [C3SE Alvis](#) partially funded by the Swedish Research Council through grant agreement no. 2022-06725.

References

- [1] David Berthelot, Nicholas Carlini, Ekin D Cubuk, Alex Kurakin, Kihyuk Sohn, Han Zhang, and Colin Raffel. Remixmatch: Semi-supervised learning with distribution alignment and augmentation anchoring. *arXiv preprint arXiv:1911.09785*, 2019. 2, 4
- [2] David Berthelot, Nicholas Carlini, Ian Goodfellow, Nicolas Papernot, Avital Oliver, and Colin A Raffel. Mixmatch: A holistic approach to semi-supervised learning. *Advances in neural information processing systems*, 32, 2019. 4, 5
- [3] Holger Caesar, Varun Bankiti, Alex H Lang, Sourabh Vora, Venice Erin Liong, Qiang Xu, Anush Krishnan, Yu Pan, Giancarlo Baldan, and Oscar Beijbom. nuscenes: A multimodal dataset for autonomous driving. In *IEEE Conference on Computer Vision and Pattern Recognition (CVPR)*, pages 11621–11631, 2020. 7
- [4] Nicolas Carion, Francisco Massa, Gabriel Synnaeve, Nicolas Usunier, Alexander Kirillov, and Sergey Zagoruyko. End-to-end object detection with transformers. In *European conference on computer vision*, pages 213–229. Springer, 2020. 3
- [5] Mathilde Caron, Hugo Touvron, Ishan Misra, Hervé Jégou, Julien Mairal, Piotr Bojanowski, and Armand Joulin. Emerging properties in self-supervised vision transformers. In *Proceedings of the IEEE/CVF international conference on computer vision*, pages 9650–9660, 2021. 2
- [6] Jiacheng Chen, Yuefan Wu, Jiaqi Tan, Hang Ma, and Yasutaka Furukawa. Maptracker: Tracking with strided memory fusion for consistent vector hd mapping. *arXiv preprint arXiv:2403.15951*, 2024. 3
- [7] Mu Chen, Zhedong Zheng, and Yi Yang. Transferring to real-world layouts: A depth-aware framework for scene adaptation, 2024. 3
- [8] Shaoyu Chen, Tianheng Cheng, Xinggong Wang, Wenming Meng, Qian Zhang, and Wenyu Liu. Efficient and robust 2d-to-bev representation learning via geometry-guided kernel transformer, 2022. 7
- [9] Ting Chen, Simon Kornblith, Mohammad Norouzi, and Geoffrey Hinton. A simple framework for contrastive learning of visual representations. In *International conference on machine learning*, pages 1597–1607. PMLR, 2020. 2
- [10] Xinlei Chen and Kaiming He. Exploring simple siamese representation learning. In *Proceedings of the IEEE/CVF conference on computer vision and pattern recognition*, pages 15750–15758, 2021. 2
- [11] Ekin D Cubuk, Barret Zoph, Jonathon Shlens, and Quoc V Le. Randaugment: Practical automated data augmentation with a reduced search space. In *Proceedings of the IEEE/CVF conference on computer vision and pattern recognition workshops*, pages 702–703, 2020. 2
- [12] Terrance DeVries and Graham W Taylor. Improved regularization of convolutional neural networks with cutout. *arXiv preprint arXiv:1708.04552*, 2017. 2, 4, 5
- [13] Hao Dong, Xianjing Zhang, Jintao Xu, Rui Ai, Weihao Gu, Huimin Lu, Juho Kannala, and Xieyuanli Chen. Superfusion: Multilevel lidar-camera fusion for long-range hd map generation. In *Proceedings of the IEEE International Conference on Robotics and Automation (ICRA)*, 2023. 3, 5
- [14] Geoff French, Samuli Laine, Timo Aila, Michal Mackiewicz, and Graham Finlayson. Semi-supervised semantic segmentation needs strong, varied perturbations. *The British Machine Vision Conference*, 2020. 2
- [15] Shuang Gao, Qiang Wang, and Yuxiang Sun. S2g2: Semi-supervised semantic bird-eye-view grid-map generation using a monocular camera for autonomous driving. *IEEE Robotics and Automation Letters*, 7(4):11974–11981, 2022. 2, 5, 6
- [16] Nikhil Gosala, Kürsat Petek, Paulo LJ Drews-Jr, Wolfram Burgard, and Abhinav Valada. Skyeye: Self-supervised bird’s-eye-view semantic mapping using monocular frontal view images. In *Proceedings of the IEEE/CVF Conference on Computer Vision and Pattern Recognition*, pages 14901–14910, 2023.
- [17] Nikhil Gosala, Kürsat Petek, B Ravi Kiran, Senthil Yogamani, Paulo Drews-Jr, Wolfram Burgard, and Abhinav Valada. Letsmap: Unsupervised representation learning for semantic bev mapping. *European Conference on Computer Vision (ECCV)*, 2024. 2
- [18] Chuan Guo, Geoff Pleiss, Yu Sun, and Kilian Q Weinberger. On calibration of modern neural networks. In *International conference on machine learning*, pages 1321–1330. PMLR, 2017. 4
- [19] Adam W Harley, Zhaoyuan Fang, Jie Li, Rares Ambrus, and Katerina Fragkiadaki. Simple-bev: What really matters for multi-sensor bev perception? In *2023 IEEE International Conference on Robotics and Automation (ICRA)*, pages 2759–2765. IEEE, 2023. 5, 7
- [20] Kaiming He, Xiangyu Zhang, Shaoqing Ren, and Jian Sun. Deep residual learning for image recognition. In *Proceedings of the IEEE conference on computer vision and pattern recognition*, pages 770–778, 2016. 5
- [21] Kaiming He, Xinlei Chen, Saining Xie, Yanghao Li, Piotr Dollár, and Ross Girshick. Masked autoencoders are scalable vision learners. In *Proceedings of the IEEE/CVF conference on computer vision and pattern recognition*, pages 16000–16009, 2022. 2
- [22] Haruya Ishikawa, Takumi Iida, Yoshinori Konishi, and Yoshimitsu Aoki. Pct: Perspective cue training framework for multi-camera bev segmentation. *arXiv preprint arXiv:2403.12530*, 2024. 2, 3, 4, 5, 6

- [23] Dong-Hyun Lee et al. Pseudo-label: The simple and efficient semi-supervised learning method for deep neural networks. In *Workshop on challenges in representation learning, ICML*, page 896. Atlanta, 2013. 4
- [24] Gang Li, Xiang Li, Yujie Wang, Yichao Wu, Ding Liang, and Shanshan Zhang. Pseco: Pseudo labeling and consistency training for semi-supervised object detection. In *European Conference on Computer Vision*, pages 457–472. Springer, 2022. 2
- [25] Qi Li, Yue Wang, Yilun Wang, and Hang Zhao. Hdmapnet: An online hd map construction and evaluation framework. In *2022 International Conference on Robotics and Automation (ICRA)*, pages 4628–4634. IEEE, 2022. 1, 3
- [26] Bencheng Liao, Shaoyu Chen, Xinggang Wang, Tianheng Cheng, Qian Zhang, Wenyu Liu, and Chang Huang. MapTR: Structured modeling and learning for online vectorized HD map construction. In *The Eleventh International Conference on Learning Representations*, 2023. 1, 3
- [27] Bencheng Liao, Shaoyu Chen, Yunchi Zhang, Bo Jiang, Qian Zhang, Wenyu Liu, Chang Huang, and Xinggang Wang. Maptrv2: An end-to-end framework for online vectorized hd map construction, 2023. 3
- [28] Adam Lilja, Junsheng Fu, Erik Stenborg, and Lars Hammarstrand. Localization is all you evaluate: Data leakage in online mapping datasets and how to fix it. In *Proceedings of the IEEE/CVF Conference on Computer Vision and Pattern Recognition*, pages 22150–22159, 2024. 1, 3, 5, 8
- [29] Tsung-Yi Lin, Priya Goyal, Ross Girshick, Kaiming He, and Piotr Dollár. Focal loss for dense object detection. In *Proceedings of the IEEE international conference on computer vision*, pages 2980–2988, 2017. 3, 5
- [30] Carl Lindström, Georg Hess, Adam Lilja, Maryam Fatemi, Lars Hammarstrand, Christoffer Petersson, and Lennart Svensson. Are nerfs ready for autonomous driving? towards closing the real-to-simulation gap. In *Proceedings of the IEEE/CVF Conference on Computer Vision and Pattern Recognition*, pages 4461–4471, 2024. 1, 3
- [31] Xiaolu Liu, Song Wang, Wentong Li, Ruizhi Yang, Junbo Chen, and Jianke Zhu. Mgmmap: Mask-guided learning for online vectorized hd map construction. In *Proceedings of the IEEE/CVF Conference on Computer Vision and Pattern Recognition*, pages 14812–14821, 2024. 5
- [32] Yicheng Liu, Tianyuan Yuan, Yue Wang, Yilun Wang, and Hang Zhao. Vectormapnet: End-to-end vectorized hd map learning. In *International Conference on Machine Learning*, pages 22352–22369. PMLR, 2023. 3
- [33] Yen-Cheng Liu, Chih-Yao Ma, Zijian He, Chia-Wen Kuo, Kan Chen, Peizhao Zhang, Bichen Wu, Zsolt Kira, and Peter Vajda. Unbiased teacher for semi-supervised object detection. *International Conference on Learning Representations (ICLR)*, 2021. 2
- [34] William Ljungbergh, Adam Lilja, Adam Tonderski Ling, Carl Lindström, Willem Verbeke, Junsheng Fu, Christoffer Petersson, Lars Hammarstrand, Michael Felsberg, et al. Gasp: Unifying geometric and semantic self-supervised pre-training for autonomous driving. *arXiv preprint arXiv:2503.15672*, 2025. 2
- [35] Yunze Man, Liangyan Gui, and Yu-Xiong Wang. Dualcross: Cross-modality cross-domain adaptation for monocular bev perception. In *2023 IEEE/RSJ International Conference on Intelligent Robots and Systems (IROS)*, pages 10910–10917. IEEE, 2023. 8
- [36] Maxime Oquab, Timothée Darcet, Théo Moutakanni, Huy V. Vo, Marc Szafraniec, Vasil Khalidov, Pierre Fernandez, Daniel HAZIZA, Francisco Massa, Alaaeldin El-Nouby, Mido Assran, Nicolas Ballas, Wojciech Galuba, Russell Howes, Po-Yao Huang, Shang-Wen Li, Ishan Misra, Michael Rabbat, Vasu Sharma, Gabriel Synnaeve, Hu Xu, Herve Jegou, Julien Mairal, Patrick Labatut, Armand Joulin, and Piotr Bojanowski. DINOv2: Learning robust visual features without supervision. *Transactions on Machine Learning Research*, 2024. Featured Certification. 7
- [37] Lang Peng, Zhirong Chen, Zhangjie Fu, Pengpeng Liang, and Erkang Cheng. Bevsegformer: Bird’s eye view semantic segmentation from arbitrary camera rigs. In *Proceedings of the IEEE/CVF Winter Conference on Applications of Computer Vision (WACV)*, pages 5935–5943, 2023. 3
- [38] Lang Peng, Zhirong Chen, Zhangjie Fu, Pengpeng Liang, and Erkang Cheng. Bevsegformer: Bird’s eye view semantic segmentation from arbitrary camera rigs. In *Proceedings of the IEEE/CVF Winter Conference on Applications of Computer Vision*, pages 5935–5943, 2023. 3
- [39] Jonah Philion and Sanja Fidler. Lift, splat, shoot: Encoding images from arbitrary camera rigs by implicitly unprojecting to 3d. In *Computer Vision—ECCV 2020: 16th European Conference, Glasgow, UK, August 23–28, 2020, Proceedings, Part XIV 16*, pages 194–210. Springer, 2020. 3, 5, 7
- [40] Zequn Qin, Jingyu Chen, Chao Chen, Xiaozhi Chen, and Xi Li. Unifusion: Unified multi-view fusion transformer for spatial-temporal representation in bird’s-eye-view. In *Proceedings of the IEEE/CVF international conference on computer vision*, pages 8690–8699, 2023. 1, 3
- [41] Kihyuk Sohn, David Berthelot, Nicholas Carlini, Zizhao Zhang, Han Zhang, Colin A Raffel, Ekin Dogus Cubuk, Alexey Kurakin, and Chun-Liang Li. Fixmatch: Simplifying semi-supervised learning with consistency and confidence. *Advances in neural information processing systems*, 33:596–608, 2020. 2, 4, 5, 6
- [42] Carole H Sudre, Wenqi Li, Tom Vercauteren, Sebastien Ourselin, and M Jorge Cardoso. Generalised dice overlap as a deep learning loss function for highly unbalanced segmentations. In *Deep Learning in Medical Image Analysis and Multimodal Learning for Clinical Decision Support: Third International Workshop, DLMIA 2017, and 7th International Workshop, ML-CDS 2017, Held in Conjunction with MICCAI 2017, Québec City, QC, Canada, September 14, Proceedings 3*, pages 240–248. Springer, 2017. 3
- [43] Antti Tarvainen and Harri Valpola. Mean teachers are better role models: Weight-averaged consistency targets improve semi-supervised deep learning results. *Advances in neural information processing systems*, 30, 2017. 2, 4
- [44] Wilhelm Tranheden, Viktor Olsson, Juliano Pinto, and Lennart Svensson. Dacs: Domain adaptation via cross-domain mixed sampling. In *Proceedings of the IEEE/CVF*

- winter conference on applications of computer vision, pages 1379–1389, 2021. 3
- [45] Vikas Verma, Kenji Kawaguchi, Alex Lamb, Juho Kannala, Arno Solin, Yoshua Bengio, and David Lopez-Paz. Interpolation consistency training for semi-supervised learning. *Neural Networks*, 145:90–106, 2022. 2
- [46] Erik Wallin, Lennart Svensson, Fredrik Kahl, and Lars Hammarstrand. Doublematch: Improving semi-supervised learning with self-supervision. In *2022 26th International Conference on Pattern Recognition (ICPR)*, pages 2871–2877. IEEE, 2022. 2, 6
- [47] Xiao Wang, Daisuke Kihara, Jiebo Luo, and Guo-Jun Qi. Enact: A self-trained framework for semi-supervised and supervised learning with ensemble transformations. *IEEE Transactions on Image Processing*, 30:1639–1647, 2021. 2
- [48] Yidong Wang, Hao Chen, Qiang Heng, Wenxin Hou, Yue Fan, Zhen Wu, Jindong Wang, Marios Savvides, Takahiro Shinozaki, Bhiksha Raj, et al. Freematch: Self-adaptive thresholding for semi-supervised learning. *International Conference on Learning Representations (ICLR)*, 2023. 2
- [49] Benjamin Wilson, William Qi, Tanmay Agarwal, John Lambert, Jagjeet Singh, Siddhesh Khandelwal, Bowen Pan, Ratnesh Kumar, Andrew Hartnett, Jhony Kaesemodel Pontes, Deva Ramanan, Peter Carr, and James Hays. Argoverse 2: Next generation datasets for self-driving perception and forecasting. In *Proceedings of the Neural Information Processing Systems Track on Datasets and Benchmarks (NeurIPS Datasets and Benchmarks)*, 2021. 5, 7
- [50] Enze Xie, Zhiding Yu, Daquan Zhou, Jonah Philion, Anima Anandkumar, Sanja Fidler, Ping Luo, and Jose M Alvarez. M²bev: Multi-camera joint 3d detection and segmentation with unified birds-eye view representation. *arXiv preprint arXiv:2204.05088*, 2022. 3
- [51] Mengde Xu, Zheng Zhang, Han Hu, Jianfeng Wang, Lijuan Wang, Fangyun Wei, Xiang Bai, and Zicheng Liu. End-to-end semi-supervised object detection with soft teacher. In *Proceedings of the IEEE/CVF international conference on computer vision*, pages 3060–3069, 2021. 2
- [52] Lihe Yang, Lei Qi, Litong Feng, Wayne Zhang, and Yinghuan Shi. Revisiting weak-to-strong consistency in semi-supervised semantic segmentation. In *Proceedings of the IEEE/CVF Conference on Computer Vision and Pattern Recognition*, pages 7236–7246, 2023. 2, 3, 4, 5
- [53] Sangdoon Yun, Dongyoon Han, Seong Joon Oh, Sanghyuk Chun, Junsuk Choe, and Youngjoon Yoo. Cutmix: Regularization strategy to train strong classifiers with localizable features. In *Proceedings of the IEEE/CVF international conference on computer vision*, pages 6023–6032, 2019. 2
- [54] Xiaohua Zhai, Avital Oliver, Alexander Kolesnikov, and Lucas Beyer. S4l: Self-supervised semi-supervised learning. In *Proceedings of the IEEE/CVF International Conference on Computer Vision (ICCV)*, 2019. 2
- [55] Bowen Zhang, Yidong Wang, Wenxin Hou, Hao Wu, Jindong Wang, Manabu Okumura, and Takahiro Shinozaki. Flexmatch: Boosting semi-supervised learning with curriculum pseudo labeling. *Advances in Neural Information Processing Systems*, 34:18408–18419, 2021. 2
- [56] Yunpeng Zhang, Zheng Zhu, Wenzhao Zheng, Junjie Huang, Guan Huang, Jie Zhou, and Jiwen Lu. Beverse: Unified perception and prediction in birds-eye-view for vision-centric autonomous driving. *arXiv preprint arXiv:2205.09743*, 2022. 3
- [57] Zhixin Zhang, Yiyuan Zhang, Xiaohan Ding, Fusheng Jin, and Xiangyu Yue. Online vectorized hd map construction using geometry. *arXiv preprint arXiv:2312.03341*, 2023. 3
- [58] Zhen Zhao, Lihe Yang, Sifan Long, Jimin Pi, Luping Zhou, and Jingdong Wang. Augmentation matters: A simple-yet-effective approach to semi-supervised semantic segmentation. In *Proceedings of the IEEE/CVF conference on computer vision and pattern recognition*, pages 11350–11359, 2023. 2, 4
- [59] Brady Zhou and Philipp Krähenbühl. Cross-view transformers for real-time map-view semantic segmentation. In *Proceedings of the IEEE/CVF conference on computer vision and pattern recognition*, pages 13760–13769, 2022. 7
- [60] Junyu Zhu, Lina Liu, Yu Tang, Feng Wen, Wanlong Li, and Yong Liu. Semi-supervised learning for visual bird’s eye view semantic segmentation. In *ICRA*, 2024. 2, 6
- [61] Yang Zou, Zhiding Yu, Xiaofeng Liu, BVK Kumar, and Jinsong Wang. Confidence regularized self-training. In *Proceedings of the IEEE/CVF international conference on computer vision*, pages 5982–5991, 2019. 3, 4

Exploring Semi-Supervised Learning for Online Mapping

Supplementary Material

6. Exact numbers

For completeness, we also show the exact performance numbers for the results shown in Figures in Sec. 4. For thresholds and temperatures, the numbers are displayed in Tab. 5 and Tab. 6 for 2.5% of the labels, respectively. For 10%, we refer to Tab. 7 and Tab. 8. In addition to these, the performance for feature similarity loss with different weights is shown in Tab. 9 and Tab. 10 for 2.5% and 10% label utilisation, respectively. The validation performance for teacher fusion over various ranges is provided in Tab. 11 and Tab. 12 for 2.5% and 10% label utilisation. We also experiment with the amount of samples to use in addition to the center sample in Tab. 13. For the test performance across multiple label utilisations, the numbers for both Argoverse 2 (AV2) and nuScenes are shown in Tab. 14. Finally, Tab. 15 provides the performance for city adaptation for both Argoverse 2 and nuScenes when varying the amount of unlabelled data.

Table 5. Validation performance (mIoU) for different thresholds on Argoverse 2 2.5% of the labels utilised.

Thresholds	0.55	0.6	0.65	0.7	0.75	0.8	0.85	0.9
Thr.	24.1	26.8	25.9	23.6	25.7	23.6	24.6	22.3
Thr.+Hard	24.4	26.6	25.2	25.5	24.2	25.0	23.7	24.6

Table 6. Validation performance (mIoU) for using sharpening with different temperatures on Argoverse 2 2.5% of the labels utilised.

Temperature	0.05	0.1	0.25	0.5	0.75	0.95
No Thr.	27.6	25.3	27.4	27.1	27.0	26.1
Thr.	24.3	26.2	27.4	25.3	25.7	26.2
Thr.+Hard	24.2	25.1	25.3	26.3	26.9	24.4

Table 7. Validation performance (mIoU) for different thresholds on Argoverse 2 10% of the labels utilised.

Thresholds	0.55	0.6	0.65	0.7	0.75	0.8	0.85	0.9
Thr.	33.6	33.9	33.4	33.3	33.0	32.4	32.1	30.9
Thr.+Hard	34.8	34.7	34.4	33.7	33.3	32.3	31.4	31.4

Table 8. Validation performance (mIoU) for using sharpening with different temperatures on Argoverse 2 10% of the labels utilised.

Temperature	0.05	0.1	0.25	0.5	0.75	0.95
No Thr.	35.0	34.8	34.9	34.7	33.8	34.6
Thr.	34.2	35.3	34.8	34.2	32.9	33.5
Thr.+Hard	34.6	34.8	34.4	34.9	33.9	34.1

Table 9. Validation performance (mIoU) for feature similarity loss with different weights on Argoverse 2 2.5% of the labels utilised.

Weight	0.05	0.1	0.25	0.5	1.0	1.5	2.0	2.5
MSE-pre	24.3	25.4	26.0	22.2	23.3	20.0	23.1	22.5
MSE-post	24.3	22.5	22.5	23.1	24.3	22.5	23.4	24.1
COS-pre	25.3	25.3	24.8	25.0	23.4	24.9	24.6	22.9
COS-post	23.4	25.1	23.4	23.6	25.5	26.1	24.4	25.4

Table 10. Validation performance (mIoU) for feature similarity loss with different weights on Argoverse 2 10% of the labels utilised.

Weight	0.05	0.1	0.25	0.5	1.0	1.5	2.0	2.5
MSE-pre	33.7	32.8	32.3	32.5	32.4	30.0	28.8	24.1
MSE-post	33.6	33.4	32.3	31.9	31.2	29.3	28.0	28.0
COS-pre	34.4	33.8	34.4	34.4	34.1	33.8	34.4	33.2
COS-post	34.0	34.8	35.4	35.1	34.4	34.8	33.4	31.4

Table 11. Validation performance (mIoU) for teacher fusion over various ranges on Argoverse 2 2.5% of the labels utilised.

Ranges	10	15	20	25	30	35	40
Probs.	27.7	27.7	27.2	27.6	28.4	28.7	26.8
Probs.+Thr.	25.5	25.9	27.3	28.2	26.9	27.5	26.7
Feats.	24.1	25.6	24.8	23.6	23.1	25.8	26.2
Feats.+Thr.	26.5	26.6	27.0	26.5	26.1	26.7	25.6

Table 12. Validation performance (mIoU) for teacher fusion over various ranges on Argoverse 2 10% of the labels utilised.

Ranges	10	15	20	25	30	35	40
Probs.	36.2	35.5	36.5	36.1	35.5	35.8	35.9
Probs.+Thr.	35.9	36.2	36.4	35.4	35.7	35.8	36.0
Feats.	34.0	34.5	34.2	34.4	34.3	34.0	34.4
Feats.+Thr.	34.2	34.0	34.8	34.1	34.4	35.4	34.6

Table 13. Multi-step Fusion with varying numbers of additional samples within a 20m range using 10% of labels. The best results are achieved with 4 additional samples.

	Additional samples		
	2	4	6
Probs	34.6	35.0	30.2
Feats	32.4	32.8	26.1

Table 14. Test performance (mIoU) for multiple label utilisations for both Argoverse 2 (AV2) and nuScenes (nuSc).

	+Unlbl Data	Label utilisation					
		2.5%	5%	10%	25%	50%	100%
AV2	✗	7.5 \pm 0.9	9.4 \pm 0.1	10.6 \pm 0.2	23.4 \pm 0.5	33.8 \pm 0.7	40.2 \pm 0.7
	✓	28.9 \pm 1.2	33.8 \pm 0.6	36.7 \pm 0.9	37.4 \pm 0.8	39.6 \pm 0.3	–
nuSc	✗	5.6 \pm 0.3	7.2 \pm 2.3	16.6 \pm 3.0	24.5 \pm 2.2	27.4 \pm 2.7	28.6 \pm 2.4
	✓	15.5 \pm 1.2	22.0 \pm 1.6	25.1 \pm 1.9	27.4 \pm 1.8	27.8 \pm 2.8	–

Table 15. Performance (mIoU) for city adaptaion for both Argoverse 2 and nuScenes when increasing amount of unlabelled data.

	Folds	# unlabelled target sequences					Using target labels
		0	25	50	100	200	
AV2	PIT-MIA \rightarrow Rest	33.6	34.4	35.5	37.5	37.2	38.9
	MIA-Rest \rightarrow PIT	36.3	38.7	40.0	40.2	40.7	41.2
	PIT-Rest \rightarrow Mia	34.5	36.1	37.5	37.8	38.5	40.2
nuSc	Boston \rightarrow Singapore	11.1	12.6	15.3	17.0	17.7	27.0